# Conformational Analysis of Poly(methylene sulfide) and Its Oligomeric Model Compounds: Anomeric Effect and Electron Flexibility of Polythioacetal

**Misa Sawanobori[†] and Yuji Sasanuma***

*Department of Materials Technology, Faculty of Engineering, Chiba University, 1-33 Yayoi-cho, Inage-ku, Chiba 263-8522, Japan*

**Akira Kaito**

*Macromolecular Technology Research Center, National Institute of Advanced Industrial Science and Technology (AIST), 1-1 Higashi, Tsukuba, Ibaraki 305-8565, Japan*

*Received June 1, 2001; Revised Manuscript Received August 20, 2001*

ABSTRACT: Conformational characteristics of poly(methylene sulfide) (PMS) and its oligomeric model compounds have been investigated. Carbon-13 NMR measurements for a dimeric model compound, bis(methylthio)methane, in the gas phase as well as in solutions were carried out, and the first-order interaction energy $E_\sigma$ representing the gauche stabilization of the C−S bond was determined from observed vicinal C−H coupling constants. For example, the $E_\sigma$ value for the gaseous dimer was evaluated as $-1.43 \pm 0.01$ kcal mol$^{-1}$, being in good agreement with the ab initio molecular orbital calculation ($-1.38$ kcal mol$^{-1}$) at the B3LYP/6-311+G(2d,p)//B3LYP/6-31G(d) level. The conformational energy $E_\sigma$ showed solvent dependence; polar solvents stabilize the trans conformation, in which dipole moments are parallel to each other and hence the molecule becomes polar. The characteristic ratio, dipole moment ratio, and configurational entropy of unperturbed PMS were estimated by the rotational isomeric state scheme and compared with those of poly(methylene oxide) (PMO). The PMS chain was indicated to be more flexible than PMO. The difference in melting point between PMS (245 °C) and PMO (180 °C) was suggested to come mainly from that in enthalpy ($\Delta H_u$) of fusion: $\Delta H_u$(PMS) > $\Delta H_u$(PMO). The geometrical parameters, electron densities, and atomic charges of trimers of PMS and PMO, obtained from the MO calculations, showed that the gauche stability in the C−S bond of the PMS homologues comes partly from antiparallel dipole−dipole interaction and $n_S \rightarrow \sigma^*_{C-S}$ hyperconjugation formed in the gauche state, partly from steric S···S repulsion occurring in the trans form. It was also shown that sulfur electrons have such flexibility as to reduce the S···S repulsion and unfavorable (parallel) dipole−dipole interaction.

## 1. Introduction

It is well-known that the alkoxy substituent at the C-2 site of pyranose ring prefers the axial (gauche) to the equatorial (trans) form (Scheme 1, X = O).[1] The gauche stabilization has been estimated to be about $-0.9$ kcal mol$^{-1}$ in free energy ($\Delta G$).[2] This phenomenon designated as the anomeric effect is a most familiar topic in stereochemistry.[3,4] Two main causes of the anomeric effect have been proposed: (1) Dipole−dipole interaction between the C−O bonds of the pyranose ring and alkoxy substituent; the gauche state with smaller resultant dipole moment is more stable.[1] (2) Delocalization of lone pair electrons ($n_O$) of the oxygen atom by a hyperconjugation ($n_O \rightarrow \sigma^*_{C-O}$) with the antibonding orbital ($\sigma^*_{C-O}$);[5] the gauche conformation, in which the lone pair is antiperiplanar to the acceptor C−O bond, is stabilized (Scheme 1).[3] The former interpretation is rationalized by the explicit solvent dependence of $\Delta G$; the trans state with a larger dipole moment becomes more populated with increasing polarity of solvent.[6] The latter has been supported by the following facts: the

**Scheme 1**

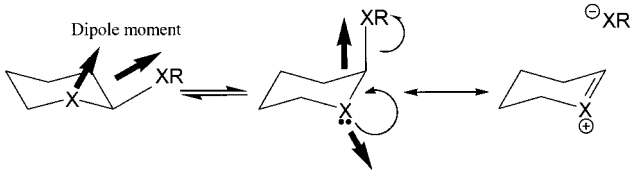


shorter O−C bond of the pyranose ring and the longer C−O bond of the alkoxy substituent in the gauche (axial) form than in the trans (equatorial) form.[4,7−9] The concept of the anomeric effect, introduced to carbohydrates, has been extended to all compounds having X−C−Y bond sequences, where X and Y are electronegative atoms such as O, S, F, and Cl.[4]

2-Alkylthiotetrahydrothiopyrans (Scheme 1, X = S) also show the anomeric effect;[6,10,11] the $\Delta G$ values have been estimated to be $-0.42$ to 0.00 kcal mol$^{-1}$, being larger than those of 2-alkoxyltetrahydropyrans (X = O). Thus, sulfur may be less effective in the gauche (axial) stability than oxygen. The natural bond orbital analysis has been attempted for $CH_2(OH)_2$, $CH_2(SH)_2$, $CH_2(SeH)_2$, and $CH_2(TeH)_2$ and reached the following conclusions.[12] The $n_X \rightarrow \sigma^*_{C-X}$ (X = O, S, Se, and Te) interactions are much contributory for $CH_2(OH)_2$ but less effective for $CH_2(SH)_2$, $CH_2(SeH)_2$, and $CH_2(TeH)_2$. The smaller anomeric effects of the higher homologues

[†] Present address: The Corporate Research and Development Center, Toshiba Corporation, 1, Komukai, Toshiba-cho, Saiwai-ku, Kawasaki 212-8582, Japan.

* To whom correspondence should be addressed. E-mail sasanuma@planet.tc.chiba-u.ac.jp; FAX +81 43 290 3394.

10.1021/ma0109525 CCC: $20.00 
Published on Web 10/12/2001

are probably due to other factors such as steric and electrostatic interactions, which stabilize the trans form in the order of O < S < Se < Te.

The simplest polymeric chain having the O−C−O−C bond sequence may be poly(methylene oxide) $[-CH_2O-]_x$ (PMO). This polymer has been widely used as engineering thermoplastics, because of its high crystallinity, superior lubricity properties, and good chemical resistance. The melting point ranges from 165 to 184 °C.[13,14] In the crystal, the PMO chain adopts a 29/16 helical structure,[15] in which all C−O bonds are in the gauche conformation. Because PMO is soluble in small number of organic solvents, the conformational analysis has mostly been carried out for model compounds,[16−21] and the conformational energy $E_\sigma$ representing the gauche stability relative to the trans state in the C−O bond has been estimated as −1.4,[18] −1.5,[16,17] −2.5,[20,21] or −3.08 to −3.38[19] kcal mol$^{-1}$.

Poly(methylene sulfide) $[-CH_2S-]_x$ (PMS) takes a 17/9 helical structure of the all-gauche conformation in the crystal.[22] This polymer is insoluble in almost all organic solvents and melts around 220−260 °C;[23,24] therefore, no quantity representing the $\theta$ state has been reported. The S−C−S−C bond sequence has been implanted in other polymeric chains to derive the first-order interaction energy $E_\sigma$ of the C−S bond. Dipole moment measurements for poly(1,3-dithiocane)[26] and poly(thiomethylene-1,4-*trans*-cyclohexylenemethylenethiomethylene)[27] gave the $E_\sigma$ values of ca. −1.2 kcal mol$^{-1}$. Thus, PMS seems to exhibit a weaker gauche preference than PMO.

In this study, we analyzed $^{13}$C NMR vicinal C−H coupling constants observed from a dimeric model compound of PMS, bis(methylthio)methane, in the gas phase and solutions to evaluate the $E_\sigma$ values, and carried out ab initio MO calculations for the oligomeric models to obtain the conformational free energies, geometrical parameters, dipole moments, atomic charges, and electron density distributions. By comparison between the observed and calculated $E_\sigma$'s, the reliability of the MO calculations was confirmed. Using the conformational energies thus established, we calculated configuration-dependent quantities such as the characteristic ratio and dipole moment ratio for the $\theta$ state and the configurational entropy change on melting. The similar theoretical treatments were also carried out for model compounds of PMO.

In this paper, the conformational characteristics and the anomeric effect of PMS are discussed in comparison with those of PMO. Here, oligomeric model compounds of PMS and PMO are respectively designated as PMS-*x* and PMO-*x*, where *x* is the degree of polymerization, viz., the number of heterogeneous atoms X's (X = S or O) included (see Figure 1): dimers, bis(methylthio)-methane (PMS-2) and dimethoxymethane (PMO-2); trimers, bis[(methylthio)methyl]sulfide (PMS-3) and 1,3-dimethoxydimethyl ether (PMO-3); tetramers, bis-[(methylthio)methylthio]methane (PMS-4) and bis-[(methoxy)methoxy]methane (PMO-4).

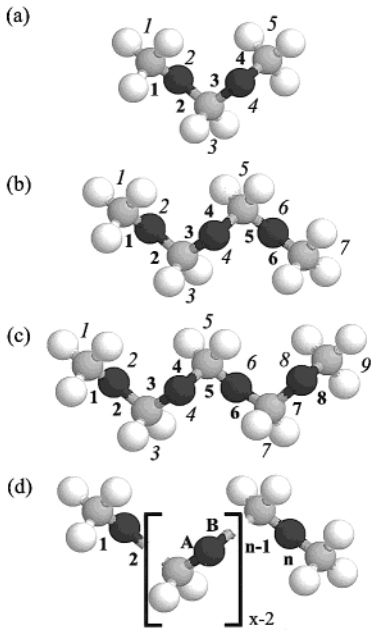


**Figure 1.** Schematic representation of compounds treated in this study: (a) dimers, bis(methylthio)methane (PMS-2) and dimethoxymethane (PMO-2); (b) trimers, bis[(methylthio)-methyl]sulfide (PMS-3) and 1,3-dimethoxydimethyl ether (PMO-3); (c) tetramer, bis[(methylthio)methylthio]methane (PMS-4) and bis[(methoxy)methoxy]methane (PMO-4); (d) polymers, PMS and PMO. The bonds and atoms (atomic groups) are numbered as indicated, and *x* is the degree of polymerization.

## 2. Materials and Methods

**2.1. Sample Preparation. 2.1.1. Bis(methylthio)-methane-$^{13}C$ (PMS-2-$^{13}C$, $^{13}CH_3SCH_2SCH_3$).**[28] Thiourea (40 g, 0.52 mol) was added through a dropping funnel to chloromethyl methyl sulfide (50 g, 0.51 mol) in a four-necked flask equipped with a mechanical stirrer, a thermometer, and a condenser. The mixture was heated at 100 °C for 1 h and at 120 °C for 8 h. After being cooled to room temperature, the reaction mixture was neutralized with sodium hydroxide (5 N), stirred at room temperature for 4 h, and filtrated. The filtrate was subjected to extraction with ether. The ethereal solution was distilled to yield 2-thiapropanethiol (bp 51 °C at 35 mmHg).

Aqueous solution of sodium hydroxide (15 wt %, 50 mL), trioctylmethylammonium chloride (1.0 g), and methyl iodide-$^{13}C$ (6.7 mL, 0.10 mol) was added under nitrogen to 2-thiapropanethiol (7.9 mL, 0.09 mol) in a four-necked flask equipped with a thermometer and a condenser. The mixture was stirred at room temperature for 1 h and heated at 90 °C for 3 h. After being cooled to room temperature, the product was extracted with ether. The organic extract was distilled to give PMS-2-$^{13}C$ (bp 60 °C at 34 mmHg, 4.9 g, 45 mmol). The total yield was 19%.

**2.1.2. 2-Methyl-1,3,5-trithiane (MTT).**[29] The starting material (1,3,5-trithiane) and solvents (toluene and tetrahydrofuran (THF)) were purified as follows. Trithiane was continuously extracted, recrystallized with toluene, and dried at room temperature under reduced pressure. Toluene was washed with sulfuric acid, dried over calcium hydride, and distilled. Tetrahydrofuran was dried over calcium hydride and lithium aluminum hydride and distilled.

Trithiane (2.7 g, 20 mmol) was added under argon to THF (100 mL) in a four-necked flask equipped with a thermometer, and the mixture was cooled to −17 °C. After *n*-butyllithium (1.5 M in hexane, 14 mL) was added dropwise, the solution was stirred at −17 °C for 1.5 h, and methyl iodide (1.4 mL, 22 mmol) was mixed in at 0 °C. After being stirred at 0 °C for 20 h and warmed to room temperature, the solution was acidified with hydrochloric acid and concentrated. The residue was extracted with ether. The ethereal layer was neutralized with sodium hydrogen carbonate solution and washed with water. The mixture was continuously extracted with ether for 24 h. The organic extract was dried over potassium carbonate, filtered, and concentrated. The crude product was recrystallized with methanol and dried at room temperature under reduced pressure to give MTT (2.5 g, 16 mmol, 81%).

**2.2. $^{13}$C NMR Measurements.** Carbon-13 NMR spectra of solution samples were measured at 125.65 MHz on a JEOL

JNM-LA500 spectrometer equipped with a variable temperature controller. During the measurement the probe temperature was maintained within ±0.1 °C fluctuations. In the measurements, free induction decays were accumulated 16 times for PMS-2-$^{13}C$ or ca. 6000 times for MTT by using the gated decoupling technique. The $\pi/2$ pulse width, data acquisition time, and recycle delay were 5.8 $\mu$s, 3.0 s, and 2.5 s, respectively. The solvents were cyclohexane-$d_{12}$, benzene-$d_6$, methanol-$d_4$, chloroform-$d_1$, and dimethyl sulfoxide-$d_6$, and the internal standard was tetramethylsilane. The concentrations of PMS-2-$^{13}C$ and MTT were 5 vol % and 25 mg/0.50 mL, respectively.

Carbon-13 NMR spectra of gaseous PMS-2-$^{13}C$ were measured at 180 °C and 67.8 MHz on a JEOL GSX-270 spectrometer equipped with a variable temperature controller. About a thousand of free induction decays were averaged using the gated decoupling technique. The $\pi/2$ pulse width, data acquisition time, and recycle delay were 4.0 $\mu$s, 1.8 s, and 1.2 s, respectively. The NMR sample was prepared as follows. About 2 $\mu$L of PMS-2-$^{13}C$ was injected into a standard 3 mm o.d. tube, which was sealed at a height of ca. 4 cm from the bottom. Placed in a 5 mm o.d. tube was the 3 mm tube, of which top was fixed with a Teflon plug. Between the inner and outer tubes, dimethyl sulfoxide-$d_6$ was filled up to the Teflon plug for $^2$H field-frequency lock. The outer tube was also sealed.

**2.3. Conformational Free Energy.** Ab initio MO calculations were carried out for PMS-2, PMS-3, PMS-4, PMO-2, PMO-3, and PMO-4 using the Gaussian 98 program[30] installed on a Compaq XP1000 workstation. At the B3LYP/6-31G(d) level, the geometries were fully optimized, and the zero-point energies, thermal energies, and entropies were also calculated. Then a scale factor of 0.9804 was used to correct for the frequency overestimation.[31,32] With the geometries determined, the self-consistent-field (SCF) energies were calculated at the B3LYP/6-311+G(2d,p) level, and atomic charges and dipole moments were computed by the Merz−Singh−Kollman method.[33,34] The conformational free energies of the individual conformations at 298.15 K and 1.0 atm were evaluated from the SCF energy, thermal energy, and entropy.

For comparison with the $^{13}$C NMR experiment for gaseous PMS-2-$^{13}C$, the conformational free energies at 453.15 K (180 °C) and 3.6 atm[35] were calculated in the same way as above.

**2.4. Configurational Entropy.** The configurational entropies per mole of skeletal bonds of PMS and PMO were calculated from[36−40]

$$S_{\text{conf}} = R\left(\ln z + T\frac{\mathrm{d}\ln z}{\mathrm{d}T}\right) \tag{1}$$

where $z$ is the configurational partition function per skeletal bond, given by

$$z = Z^{1/n} \tag{2}$$

with $Z$ and $n$ being the partition function of the whole chain and the number of skeletal bonds. The $Z$ function can be calculated from

$$Z = \mathbf{J}^*\left(\prod_{i=2}^{n-1} U_i\right)\mathbf{J} \tag{3}$$

where $\mathbf{J}^* = [100]$ and $\mathbf{J}$ is the $3 \times 1$ column matrix of which elements are unity. The statistical weight matrices $U_i$'s ($i$ = bond number) are scaled so that the weight of the lowest-energy conformation is unity, as given below.

## 3. Results and Discussion

**3.1. $^{13}$C NMR Data from PMS-2-$^{13}$C and MTT.** Figure 2 shows examples of $^{13}$C NMR spectra observed from the labeled methyl carbon of PMS-2-$^{13}C$ and methylene carbons of MTT. The $^{13}$C NMR signal from PMS-2-$^{13}C$ was split into four by direct couplings and further into three by vicinal couplings. For MTT, vicinal couplings of the methylene carbon with three protons (Figure 3c) produced two triplets, which indicate that the MTT ring does not flip-flop even at 70 °C.

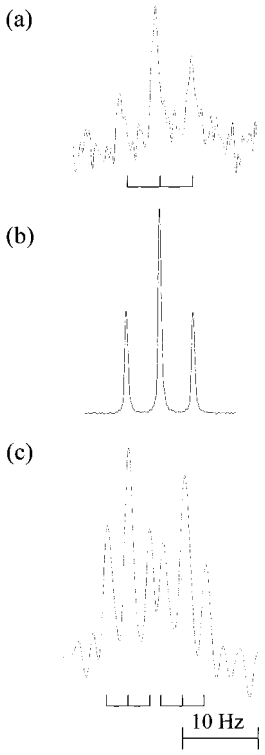


**Figure 2.** $^{13}$C NMR spectra observed from the labeled methyl carbon of PMS-2-$^{13}C$ (a) in the gas phase at 180 °C and (b) in benzene at 70 °C and (c) methylene carbons of MTT in benzene at 70 °C.

The vicinal coupling constant $^3J_{CH}$ of PMS-2-$^{13}C$ provides information regarding the conformation around the C−S bond. The observed $^3J_{CH}$ value corresponds to the average of vicinal $^{13}$C−$^1$H$_a$ and $^{13}$C−$^1$H$_b$ coupling constants (see Figure 3):

$$^3J_{CH} = \frac{^3J_{CH_a} + {}^3J_{CH_b}}{2} = \frac{2\,{}^3J_G\,p_t + {}^3J_T\,p_g + {}^3J_G\,p_g}{2} \tag{4}$$

where $p_t$ and $p_g$ are the trans and gauche fractions of the C−S bond. Therefore, the definition of the bond conformations dictates that

$$p_t + p_g = 1 \tag{5}$$

and

$$p_{g^+} = p_{g^-} = \frac{p_g}{2} \tag{6}$$

where $p_{g^+}$ and $p_{g^-}$ are the gauche+ and gauche− fractions. From these equations, we have

$$p_t = \frac{^3J_T + {}^3J_G - 2\,{}^3J_{CH}}{^3J_T - {}^3J_G} \tag{7}$$

Here the $^3J_T$ and $^3J_G$ values obtained from MTT dissolved in the corresponding solvent were used: $^3J_T$ = 7.13 ± 0.02 Hz and $^3J_G$ = 2.62 ± 0.02 Hz in benzene at 70 °C; $^3J_T$ = 7.12 ± 0.09 Hz and $^3J_G$ = 2.58 ± 0.02 Hz

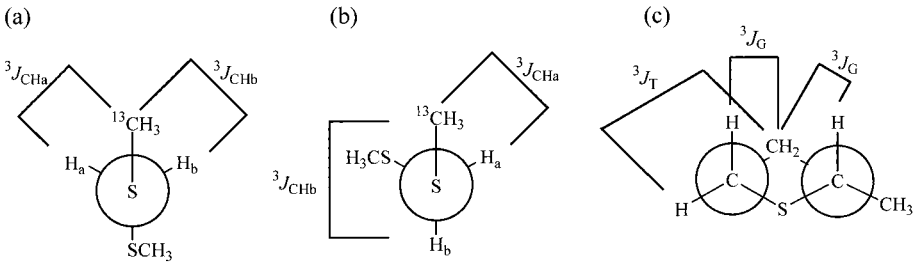


**Figure 3.** Preferred conformations around the C−S bond and definitions of $^3J_{CH_a}$, $^3J_{CH_b}$, $^3J_T$, and $^3J_G$: (a) trans and (b) gauche conformations of PMS-2-$^{13}C$ and (c) MTT.

**Table 1. Observed Vicinal $^{13}C-^1H$ Coupling Constants, C−S Bond Conformations, and Conformational Energies of PMS-2-$^{13}C$**

| medium | dielectric constant of medium[a] | temp (°C) | $^3J_{CH}$ (Hz) | $p_t$ | $p_g$ | $E_\sigma$ (kcal mol$^{-1}$) |
|---|---|---|---|---|---|---|
| gas | 1.0 | 180.0 | 4.52 ± 0.04 | 0.16 ± 0.02 | 0.84 ± 0.01 | −1.43 ± 0.01 |
| cyclohexane-$d_{12}$ | 2.02 | 15.0 | 4.64 | 0.10 | 0.90 | −1.20 |
| | | 25.0 | 4.63 | 0.11 | 0.89 | −1.21 |
| | | 40.0 | 4.62 | 0.11 | 0.89 | −1.24 |
| | | 55.0 | 4.61 | 0.12 | 0.88 | −1.27 |
| | | 70.0 | 4.59 | 0.13 | 0.87 | −1.27 |
| benzene-$d_6$ | 2.28 | 15.0 | 4.57 | 0.14 | 0.86 | −1.02 |
| | | 25.0 | 4.57 | 0.14 | 0.86 | −1.05 |
| | | 40.0 | 4.56 | 0.14 | 0.86 | −1.08 |
| | | 55.0 | 4.54 | 0.15 | 0.85 | −1.08 |
| | | 70.0 | 4.53 | 0.15 | 0.85 | −1.11 |
| chloroform-$d_1$ | 4.81 | 0.0 | 4.53 | 0.14 | 0.86 | −0.94 |
| | | 10.0 | 4.52 | 0.15 | 0.85 | −0.95 |
| | | 25.0 | 4.51 | 0.15 | 0.85 | −0.98 |
| | | 40.0 | 4.50 | 0.15 | 0.85 | −1.01 |
| | | 55.0 | 4.48 | 0.16 | 0.84 | −1.01 |
| methanol-$d_4$ | 32.6 | 0.0 | 4.59 | 0.13 | 0.87 | −0.98 |
| | | 15.0 | 4.56 | 0.15 | 0.85 | −0.97 |
| | | 25.0 | 4.55 | 0.15 | 0.85 | −0.98 |
| | | 40.0 | 4.54 | 0.15 | 0.85 | −1.00 |
| | | 55.0 | 4.48 | 0.18 | 0.82 | −0.92 |
| dimethyl sulfoxide-$d_6$ | 45.0 | 25.0 | 4.49 | 0.15 | 0.85 | −0.96 |
| | | 55.0 | 4.47 | 0.16 | 0.84 | −1.00 |
| | | 80.0 | 4.44 | 0.18 | 0.82 | −1.00 |
| | | 110.0 | 4.41 | 0.19 | 0.81 | −1.01 |
| | | 135.0 | 4.40 | 0.20 | 0.80 | −1.05 |

[a] At 20 °C.

in chloroform at 50 °C; $^3J_T = 7.27 \pm 0.05$ Hz and $^3J_G = 2.54 \pm 0.02$ Hz in methanol at 55 °C; $^3J_T = 6.92 \pm 0.07$ Hz and $^3J_G = 2.71 \pm 0.04$ Hz in dimethyl sulfoxide at 135 °C. Well-defined spectra obtained from MTT at comparatively high temperatures were employed in the analysis. Because MTT was insoluble in cyclohexane, $^3J_G$ and $^3J_T$ values obtained from the benzene solution were used for PMS-2-$^{13}C$ in the gas phase and cyclohexane. Listed in Table 1 are the $p_t$ and $p_g$ values thus evaluated, together with the experimental $^3J_{CH}$ values.[41]

According to the rotational isomeric state (RIS) scheme,[17] the statistical weight matrices $U_i$'s of PMS-2 and PMO-2 may be given as

$$U_2 = \begin{bmatrix} \sigma^{-1} & 1 & 1 \\ 0 & 0 & 0 \\ 0 & 0 & 0 \end{bmatrix} \tag{8}$$

$$U_3 = \begin{bmatrix} \sigma^{-1} & 1 & 1 \\ \sigma^{-1} & 1 & 0 \\ \sigma^{-1} & 0 & 1 \end{bmatrix} \tag{9}$$

where $\sigma$ is the statistical weight which can be related to the conformational energy $E_\sigma$ by $\sigma = \exp(-E_\sigma/RT)$. Our MO calculations showed that the $g^+g^-$ and $g^-g^+$ conformations of PMS-2 and PMO-2 are essentially absent because of severe steric repulsion between the $CH_3$ terminals; therefore, the (2,3) and (3,2) elements of $U_3$ are set to zero. From the above matrices, we have

$$p_t = \frac{2\sigma + 1}{2\sigma^2 + 4\sigma + 1} \tag{10}$$

$$p_g = \frac{2\sigma(\sigma + 1)}{2\sigma^2 + 4\sigma + 1} \tag{11}$$

The experimental $E_\sigma$ values obtained from eqs 7 and 10 are also listed in Table 1. In principle, the $E_\sigma$ value increases with increasing polarity of solvent and decreasing temperature.

**3.2. MO Calculations.** Free energies of possible conformers of PMS-2, PMS-3, PMO-2, and PMO-3, obtained from the MO calculations, are shown in Table 2. The $g^+g^-$ and $g^-g^+$ conformers of the dimers are not included for the reason described above. The free energy of each conformer is represented as the difference from that of the most stable all-gauche state.

**Table 2. Free Energies ($\Delta G_k$) of Conformers of Dimers, Trimers, and Tetramers of PMS and PMO, Evaluated by ab Initio Molecular Orbital Calculations at the B3LYP/6-311+G(2d,p)//B3LYP/6-31G(d) Level[a]**

| $k$ | conformation | $M_k$ | statistical weight(s) | $\Delta G_k$ (kcal mol$^{-1}$) PMS-$x$ | PMO-$x$ |
|---|---|---|---|---|---|
| | | | Dimer ($x = 2$) | | |
| 1 | t t | 1 | $\sigma^{-2}$ | 5.12 (5.88)[b] | 5.08 |
| 2 | t g$^+$ | 4 | $\sigma^{-1}$ | 1.54 (1.38)[b] | 2.15 |
| 3 | g$^+$g$^+$ | 2 | 1 | 0.00 (0.00)[b] | 0.00 |
| | | | Trimer ($x = 3$)[c] | | |
| 1 | t t t | 1 | $\sigma^{-4}$ | 9.66 | 9.26 |
| 2 | t t g$^+$ | 4 | $\sigma^{-3}$ | *d* | *d* |
| 3 | t g$^+$ t | 4 | $\sigma^{-3}$ | *d* | *d* |
| 4 | t g$^+$ t g$^+$ | 4 | $\sigma^{-2}$ | 2.76 | 3.35 |
| 5 | t g$^+$ t g$^-$ | 4 | $\sigma^{-2}$ | 2.94 | 3.80 |
| 6 | t g$^+$ g$^+$ t | 2 | $\sigma^{-2}$ | 2.78 | 4.03 |
| 7 | t g$^+$ g$^+$ g$^+$ | 4 | $\sigma^{-1}$ | 1.50 | 2.08 |
| 8 | t g$^+$ g$^-$ t | 2 | $\sigma^{-2}\omega$ | 6.02 | 6.46 |
| 9 | t g$^+$ g$^-$ g$^-$ | 4 | $\sigma^{-1}\omega$ | 3.28 | 3.46 |
| 10 | g$^+$ t t g$^+$ | 2 | $\sigma^{-2}$ | 2.85 | 3.96 |
| 11 | g$^+$ t t g$^-$ | 2 | $\sigma^{-2}$ | 3.16 | 4.60 |
| 12 | g$^+$ t g$^+$ g$^+$ | 4 | $\sigma^{-1}$ | 1.61 | 1.71 |
| 13 | g$^+$ g$^+$ t g$^-$ | 4 | $\sigma^{-1}$ | 1.69 | 1.57 |
| 14 | g$^+$ g$^+$ g$^+$ g$^+$ | 2 | 1 | 0.00 | 0.00 |
| 15 | g$^+$ g$^+$ g$^-$ g$^-$ | 2 | $\omega$ | 3.07 | 2.08 |
| | | | Tetramer ($x = 4$) | | |
| 1 | t g$^+$ g$^+$ g$^+$ g$^+$ | 4 | $\sigma^{-1}$ | 1.24 | 1.98 |
| 2 | g$^+$ t g$^+$ g$^+$ g$^+$ | 4 | $\sigma^{-1}$ | *d* | 1.61 |
| 3 | g$^+$ g$^+$ t g$^+$ g$^+$ | 4 | $\sigma^{-1}$ | 1.61 | 1.66 |
| 4 | g$^+$ g$^+$ g$^+$ g$^+$ g$^+$ | 2 | 1 | 0.00 | 0.00 |

[a] Relative to those of the all-gauche conformation. Calculated for the dimers, trimers, and tetramers at 298.15 K and 1 atm. [b] For comparison with $^{13}$C NMR experiment for gaseous PMS-2-$^{13}C$, the $\Delta G_k$ values for PMS-2 at 453 K and 3.6 atm are shown in the parentheses. See ref 35. [c] According to the least-squares fittings of eqs 13 and 14, the $E_\sigma$ and $E_\omega$ values were respectively determined as follows: −1.54 and 2.09 kcal mol$^{-1}$ (PMS-3) and −1.72 and 1.98 kcal mol$^{-1}$ (PMO-3). [d] The local minimum of the potential was not found by the geometrical optimization.

The statistical weight matrices for the second and third C−S bonds of PMS-3 and PMO-3 are respectively given by eqs 8 and 9, and that for the fourth bond may be expressed as

$$U_4 = \begin{bmatrix} \sigma^{-1} & 1 & 1 \\ \sigma^{-1} & 1 & \omega \\ \sigma^{-1} & \omega & 1 \end{bmatrix} \tag{12}$$

where $\omega$ is the Boltzmann factor for the second-order X···X (X = S or O) interaction occurring in the $g^{\pm}g^{\mp}$ conformations for the third and fourth C−X bond pairs. The $U_5$ of the trimers is equivalent to $U_3$. Equations 8, 9, and 12 are equivalent to statistical weight matrices employed in the previous study.[17] In the calculation of the configuration entropy, the statistical weight for the lowest-energy state, i.e., the all-gauche conformation, must be defined as unity. The conformational free energy of each conformer is given as the difference from that of the all-gauche state. Therefore, in eqs 8, 9, and 12, a weight of unity is assigned to the gauche states.

For PMS-2 and PMO-2, the free energy difference between $g^+g^+$ and $g^+t$ states may be adopted as the conformational energy $E_\sigma$: −1.54 kcal mol$^{-1}$ (PMS-2) and −2.15 kcal mol$^{-1}$ (PMO-2). In the RIS scheme, the $\Delta G$ values of PMS-3 and PMO-3 are approximated as a function of $E_\sigma$ and $E_\omega$; for example, the $\Delta G$ value of the $tg^+g^-t$ conformation may correspond to $-2E_\sigma + E_\omega$. The $E_\sigma$ and $E_\omega$ values were determined by minimizing the following function:

$$S(\boldsymbol{E}) = \frac{1}{K}\sum_k \Delta_k{}^2(\mathbf{E}) \tag{13}$$

where

$$\Delta_k{}^2(\mathbf{E}) = (\sum_\xi L(\xi)E_\xi - \Delta G_k)^2 M_k \exp(-\Delta G_k/RT) \tag{14}$$

with $K$ and $M_k$ being the total number ($=\sum_k M_k$) of conformers and the multiplicity of a conformation $k$. The function $L(\xi)$ gives the number of conformational energy $E_\xi$ ($\xi = \sigma$ or $\omega$) included in the conformation. The squared difference between $\Delta G_k$ and the sum of $E_\xi$'s is multiplied by the Boltzmann factor $\exp(-\Delta G_k/RT)$ so as to weight low-energy conformations. The temperature $T$ was set to 298.15 K. Consequently, the $E_\sigma$ and $E_\omega$ values were respectively determined as follows: −1.54 and 2.09 kcal mol$^{-1}$ (PMS-3) and −1.72 and 1.98 kcal mol$^{-1}$ (PMO-3).

**3.3. Comparison between Theory and Experiment.** Our MO calculations gave $E_\sigma$'s of −2.15 and −1.72 kcal mol$^{-1}$ for gaseous PMO-2 and PMO-3, respectively. Abe et al.[42] evaluated an $E_\sigma$ value of $-2.5 \pm 0.2$ kcal mol$^{-1}$ from $^{13}$C NMR measurements for gaseous PMO-2. From dipole moment measurements for PMO-2 and PMO-3 in *n*-hexane at 25 °C, Uchida et al.[43] evaluated the gauche energy to be −1.74 kcal mol$^{-1}$. Our MO calculations well reproduced these experimental observations. Flory[17] estimated the $E_\sigma$ and $E_\omega$ values as −1.5 and 1.8 kcal mol$^{-1}$, respectively, so as to reproduce the characteristic ratio of PMO as well as the data of Uchida et al.[43] Abe and Mark[18] offered an $E_\sigma$ value of −1.4 kcal mol$^{-1}$ for unperturbed PMO. From vibrational spectra, Sakakibara et al.[44] estimated the enthalpy difference between the tg and gg conformations of liquid PMO-2 as −1.2 kcal mol$^{-1}$. As stated above, the experimental $E_\sigma$ values of PMO-$x$'s have been found within a wide range. One reason may be the solvent effect. As has often been pointed out for the anomeric effect,[6] polar solvents stabilize the more polar (trans) conformation; i.e., the gauche preference decreases with increasing dielectric constant of solvent. The other reason may be the chain-length dependence. Our calculations indicate that the gauche stability (−2.15 kcal mol$^{-1}$) of PMO-2 exceeds that (−1.72 kcal mol$^{-1}$) of PMO-3. For PMO-4, therefore, the free energies of the $tg^+g^+g^+g^+$, $g^+tg^+g^+g^+$, and $g^+g^+tg^+g^+$ conformations were calculated (see Table 2). The $E_\sigma$ value of PMO-4 depends on the bond position; bonds 2, 3, and 4 show $E_\sigma$'s of −1.98, −1.61, and −1.66 kcal mol$^{-1}$, respectively. The outer bond seems to have a smaller $E_\sigma$ than the inner bond. This tendency can be found for PMO-3; bonds 2 ($tg^+g^+$) and 3 ($g^+tg^+$ or $g^+g^+tg^-$) have $E_\sigma$'s of −2.08 kcal mol$^{-1}$ and −1.71 or −1.57 kcal mol$^{-1}$, respectively. If the solvent and chain-length effects are taken into account, therefore, our MO calculations support Flory, Mark, and Abe's estimation[17,18] of $E_\sigma = -1.4$ to −1.5 kcal mol$^{-1}$ for unperturbed PMO. The terminal bonds of PMO probably have a smaller conformational energy than the inner bonds. However, the terminal effect is negligible in the calculations of configuration-dependent properties such as the characteristic ratio, dipole moment ratio, and configurational entropy of long chains.

**Table 3. Dipole Moments of Conformers of PMS-3**

| $k$ | conformation | $\mu_k^{MO}$ [a] (D) | $\mu_k^{BOND}$ [b] (D) |
|---|---|---|---|
| 1 | t t t t | 4.52 | 4.77 |
| 2 | t t t $g^+$ | *c* | *c* |
| 3 | t t $g^+$ t | *c* | *c* |
| 4 | t $g^+$ t $g^+$ | 2.71 | 2.81 |
| 5 | t $g^+$ t $g^-$ | 3.52 | 3.64 |
| 6 | t $g^+$ $g^+$ t | 2.39 | 2.64 |
| 7 | t $g^+$ $g^+$ $g^+$ | 1.51 | 1.09 |
| 8 | t $g^+$ $g^-$ t | 3.29 | 3.85 |
| 9 | t $g^+$ $g^-$ $g^-$ | 1.17 | 1.67 |
| 10 | $g^+$ t t $g^+$ | 1.79 | 1.45 |
| 11 | $g^+$ t t $g^-$ | 2.99 | 2.13 |
| 12 | $g^+$ t $g^+$ $g^+$ | 1.69 | 1.57 |
| 13 | $g^+$ $g^+$ t $g^-$ | 1.48 | 1.66 |
| 14 | $g^+$ $g^+$ $g^+$ $g^+$ | 1.45 | 1.52 |
| 15 | $g^+$ $g^+$ $g^-$ $g^-$ | 1.23 | 1.65 |
| RMSE,[d] D | | | 0.37 |

[a] Evaluated from ab initio MO calculations at the B3LYP/6-311+G(2d,p)//B3LYP/6-31G(d) level. [b] Estimated as the sum of bond dipole moments. The C−S bond dipole moment $m_{C-S}$ was determined by the least-squares fitting according to eq 15 to be $1.23 \pm 0.08$ D. [c] The local minimum of the potential was not found by the geometrical optimization. [d] The root-mean-square error between $\mu_k^{MO}$'s and $\mu_k^{BOND}$'s.

Our NMR analysis for gaseous PMS-2-$^{13}C$ at 180 °C and 3.6 atm gave an $E_\sigma$ value of $-1.43 \pm 0.01$ kcal mol$^{-1}$, which was closely reproduced by our MO calculation ($E_\sigma = -1.38$ kcal mol$^{-1}$). Thus, it can be concluded that the MO calculations at the B3LYP/6-311+G(2d,p)//B3LYP/6-31G(d) level provide fully quantitative data for both PMS-*x*'s and PMO-*x*'s. The MO calculations gave an $E_\sigma$ value ($-1.54$ kcal mol$^{-1}$) common to PMS-2 and PMS-3 but $\Delta G_k$'s of 1.24 and 1.61 kcal mol$^{-1}$ for the $tg^+g^+g^+g^+$ and $g^+g^+tg^+g^+g^+$ conformations of PMS-4, respectively; no explicit chain-length dependence of $E_\sigma$ can be seen for PMS-*x*'s. Both experiments and calculations show that PMS-*x*'s have somewhat weaker gauche preference than PMO-*x*'s.

As stated in the Introduction, because it is difficult to obtain experimental data on the $\theta$ state of PMS itself, other polymers including the S−C−S−C bond sequence have been subjected to conformational analysis. From dipole moments and their temperature coefficients of poly(1,3-dithiocane)[26] and poly(thiomethylene-1,4-*trans*-cyclohexylenemethylene thiomethylene)[27] in benzene, the conformational energy $E_\sigma$ was indirectly estimated to be $-1.2$ kcal mol$^{-1}$. This estimate agrees well with our NMR data ($E_\sigma = -1.02$ to $-1.11$ kcal mol$^{-1}$) for PMS-2-$^{13}C$ in benzene.

**3.4. Dipole Moment.** The C−S bond dipole moment $m_{C-S}$ was determined on the basis of the MO calculations for PMS-3; the $m_{C-S}$ value was optimized so as to minimize the *f* function

$$f(m_{C-S}) = \sum_k (\mu_k^{MO} - \mu_k^{BOND})^2 M_k \exp(-\Delta G_k/RT) \quad (15)$$

where $\mu_k^{MO}$ is the dipole moment of the conformer $k$, obtained from MO calculations, and $\mu_k^{BOND}$ is calculated from

$$\mu_k^{BOND} = m_{C-S} \sum_i \mathbf{b}_i^k \quad (16)$$

with $\mathbf{b}_i^k$ being the unit vector in the C → S direction of the $i$th bond of the conformer $k$. As a result of the optimization, the $m_{C-S}$ value was determined as $1.23 \pm 0.08$ D. Then, the root-mean-square error (RMSE) between $\mu_k^{MO}$'s and $\mu_k^{BOND}$'s was 0.37 D. In Table 3, the $\mu_k^{BOND}$ values are compared with $\mu_k^{MO}$'s. From the table, it can be seen that $\mu_k^{BOND}$'s agree fairly well with $\mu_k^{MO}$'s. This indicates that the calculation based on eq 16 is applicable to these thioacetals. The $m_{C-S}$ value obtained here is close to that (1.21 D) so far used for polysulfides.[45,46]

**Table 4. Conformational Energies and Geometrical Parameters of PMS, Used in Calculations of Characteristic Ratio, Dipole Moment Ratio, and Configurational Entropy**

| | |
|---|---|
| conformational energy, kcal mol$^{-1}$ | |
| $E_\sigma$ | $-1.05$[a] |
| $E_\omega$ | 2.09[b] |
| bond length,[c] Å | |
| C−S | 1.833 |
| bond angle,[c] deg | |
| ∠CSC | 100.06 |
| ∠SCS | 117.36 |
| dihedral angle,[c] deg | |
| $\phi_{trans}$ | 0.00 |
| $\phi_{gauche\pm}$ | ±113.07 |
| bond dipole moment, D | |
| $m_{C-S}$ | 1.23[d] |

[a] From $^{13}$C NMR observed from PMS-2-$^{13}C$ in benzene at 25.0 °C (Table 1). [b] Evaluated by the least-squares fitting for the MO free energies (Table 2) of PMS-3, according to eqs 13 and 14. See text. [c] From the all-gauche conformation of PMS-3. [d] Determined by the least-squares fitting for dipole moments (Table 3) of conformers of PMS-3, according to eqs 15.

**3.5. Configuration-Dependent Properties of PMS and PMO.** The characteristic ratio ($\langle r^2\rangle_0/nl^2$) and dipole moment ratio ($\langle\mu^2\rangle/nm^2$) of unperturbed PMS were calculated by the RIS scheme.[17] Here, $r$ is the end-to-end distance, $l$ is the bond length, $m$ is the bond dipole moment, and the angular brackets denote the ensemble average. The statistical weight matrices ($U_A$ and $U_B$) of PMS and PMO correspond to $U_3$ and $U_4$, respectively. Although the $\theta$ state of PMS is imaginary, it should be meaningful to investigate these configuration-dependent properties of PMS and compare them with those of other polymers. The conformational energies and geometrical parameters used in the calculations are listed in Table 4. In Figure 4, the $\langle r^2\rangle_0/nl^2$ and $\langle\mu^2\rangle/nm^2$ values are shown as a function of the degree of polymerization, $x$.

The characteristic ratio increases monotonically with $x$. The $\langle r^2\rangle_0/nl^2$ value calculated for $x = 300$ is 7.6. On the other hand, the dipole moment ratio decreases with increasing $x$. The $\langle\mu^2\rangle/nm^2$ value at $x = 300$ is 0.17. For PMO of $x = 300$, the conformational energies and geometrical parameters offered by Flory[47] and Abe and Mark[48] yield $\langle r^2\rangle_0/nl^2$'s of 8.0 and 9.2, respectively. The experimental $\langle r^2\rangle_0/nl^2$ values (7.5[49] and $10.5 \pm 1.5$[50]) estimated for unperturbed PMO are considerably scattered.

The configurational entropy $S_{conf}$ of PMS of $x = 300$ at 25 °C was calculated from eq 1 to be 2.7 cal mol$^{-1}$ K$^{-1}$.[51] For PMO of $x = 300$ at 25 °C, the energy parameters of Flory[47] and Abe and Mark[48] yielded $S_{conf}$'s of 2.0 and 2.3 cal mol$^{-1}$ K$^{-1}$, respectively. The melting point is given by $T_m = \Delta H_u/\Delta S_u$, where $\Delta H_u$ and $\Delta S_u$ are enthalpy and entropy of fusion. For PMO, the $\Delta S_u$ value was experimentally estimated as 3.9 cal mol$^{-1}$ K$^{-1}$,[52−54] and the melting point was 180 °C. The entropy $\Delta S_u$ of fusion can be broken down into $\Delta S_{conf}$ and $\Delta S_v$,[37,55] where $\Delta S_v = (\alpha/\beta)\Delta V_u$, with $\alpha$, $\beta$, and $\Delta V_u$ being the thermal expansion coefficient, compressibility, and

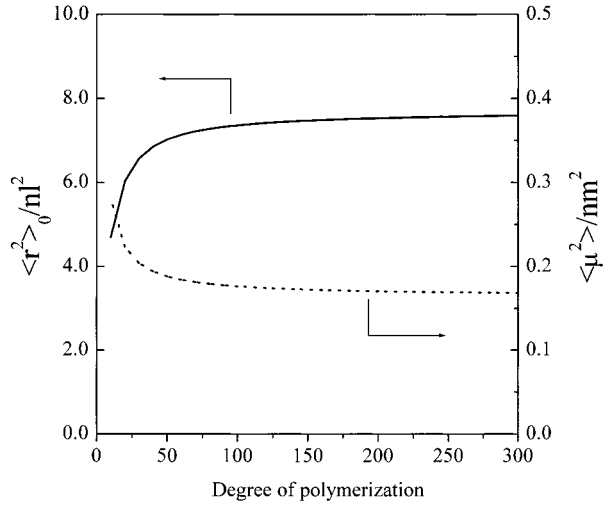


**Figure 4.** Characteristic ratio $\langle r^2\rangle_0/nl^2$ and dipole moment ratio $\langle \mu^2\rangle/nm^2$ of unperturbed PMS as a function of the degree of polymerization, $x$, calculated using the conformational energies and geometrical parameters in Table 4.

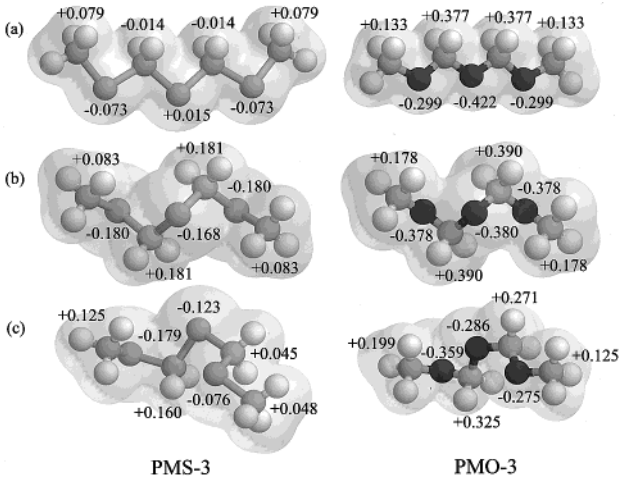


**Figure 5.** Electron density distributions and atomic charges of (a) all-trans, (b) all-gauche, and $g^+tg^+t$ conformations of PMS-3 and PMO-3. The atomic charges of hydrogens are summed into the bonded carbons.

volume change on melting, respectively. Flory's[47] and Abe and Mark's[48] parameters yield $\Delta S_{conf}$'s of 2.9 and 3.1 cal mol$^{-1}$ K$^{-1}$ for PMO at 180 °C, respectively, and a $\Delta S_{conf}$ value of 2.8 cal mol$^{-1}$ K$^{-1}$ was experimentally obtained.[56] Accordingly, the contribution of $\Delta S_{conf}$ to $\Delta S_u$ amounts to 70−80%. For PMS of $x = 300$ at the melting point (245 °C), our conformational energies (Table 4) gave a $\Delta S_{conf}$ value of 3.4 cal mol$^{-1}$ K$^{-1}$, which is larger than that of PMO. Probably, PMS has a larger $\Delta S_u$ than PMO, being more flexible in the molten state. However, PMS melts at a much higher temperature than PMO. This must be ascribed to the difference in $\Delta H_u$: $\Delta H_u$(PMS) > $\Delta H_u$(PMO). Such thermal properties of polysulfides, e.g., poly(ethylene sulfide),[40,57] have been discussed in comparison with those of polyethers.

**3.6. Electron Density Distribution, Atomic Charges, and Anomeric Effects.** Illustrated in Figure 5 are the optimized geometries of the all-trans, all-gauche, and $g^+tg^+t$ conformations of PMS-3 and PMO-3, together with the electron density distributions and atomic (group) charges obtained by the Merz−Singh−Kollman method at the B3LYP/6-311+G(2d,p) level. The bond lengths and bond angles of the conformers are listed in Table 5. The all-trans conformer of PMS-3 is curved toward the methylene groups; bond angles ∠SCS's (108.35°) are larger than ∠CSC's (98.29° and 97.30°). On the other hand, the all-trans PMO-3 is curved toward the oxygen atoms; ∠OCO's (105.74°) are smaller than ∠COC's (112.40° and 113.03°). This may be due to the difference in van der Waals radius between sulfur and oxygen (1.80 Å for S and 1.52 Å for O).[58]

**Table 5. Bond Lengths and Bond Angles of All-Trans, All-Gauche, and $g^+tg^+t$ Conformations of PMS-3 and PMO-3, Obtained from ab Initio MO Calculations at the B3LYP/6-31G(d) Level[a]**

| | conformations of bonds 2, 3, 4, and 5 | | |
|---|---|---|---|
| | tttt | $g^+g^+g^+g^+$ | $g^+tg^+t$ |
| **PMS-3** | | | |
| bond length, Å | | | |
| $C_1-S_2$ | 1.827 | 1.826 | 1.828 |
| $S_2-C_3$ | 1.835 | 1.830 | 1.819 |
| $C_3-S_4$ | 1.835 | 1.835 | 1.847 |
| $S_4-C_5$ | 1.835 | 1.835 | 1.825 |
| $C_5-S_6$ | 1.835 | 1.830 | 1.841 |
| $S_6-C_7$ | 1.827 | 1.826 | 1.830 |
| bond angle, deg | | | |
| $\angle C_1S_2C_3$ | 98.29 | 100.38 | 100.46 |
| $\angle S_2C_3S_4$ | 108.35 | 117.36 | 112.34 |
| $\angle C_3S_4C_5$ | 97.30 | 100.06 | 100.28 |
| $\angle S_4C_5S_6$ | 108.35 | 117.36 | 112.30 |
| $\angle C_5S_6C_7$ | 98.29 | 100.38 | 99.54 |
| **PMO-3** | | | |
| bond length, Å | | | |
| $C_1-O_2$ | 1.412 | 1.421 | 1.422 |
| $O_2-C_3$ | 1.394 | 1.400 | 1.385 |
| $C_3-O_4$ | 1.398 | 1.417 | 1.427 |
| $O_4-C_5$ | 1.398 | 1.417 | 1.384 |
| $C_5-O_6$ | 1.394 | 1.400 | 1.414 |
| $O_6-C_7$ | 1.412 | 1.421 | 1.413 |
| bond angle, deg | | | |
| $\angle C_1O_2C_3$ | 112.40 | 113.62 | 113.78 |
| $\angle O_2C_3O_4$ | 105.74 | 113.29 | 109.77 |
| $\angle C_3O_4C_5$ | 113.03 | 113.39 | 114.45 |
| $\angle O_4C_5O_6$ | 105.74 | 113.29 | 109.85 |
| $\angle C_5O_6C_7$ | 112.40 | 113.62 | 112.48 |

[a] For atom and bond numbers, see Figure 1.

In all-trans PMO-3, all the oxygen atoms are negatively charged because oxygen has an electronegativity (3.5) larger than carbon (2.5).[59] In all-trans PMS-3, however, the differences in charge between S and $CH_2$ are slight, and the central S atom has a positive charge of +0.015. The sulfur electrons are so flexible as to reduce the S···S repulsion and unfavorable (parallel) dipole−dipole interaction. The electronegativity of sulfur is almost the same as that of carbon.[59]

In all-gauche PMS-3, all the sulfur atoms and methylene groups have negative and positive charges, respectively. The dipole moments formed along the bisector of ∠CSC angle are canceled out and stabilize the all-gauche conformation. The all-gauche conformer has a larger S···S distance (3.13 Å) than the all-trans one (2.98 Å). These tendencies can also be found in the all-gauche PMO-3. However, magnitudes of atomic charges of PMO-3 are about twice as large as those of PMS-3. The O···O distances of the all-gauche and all-trans PMO-3's are 2.35 and 2.23 Å, respectively.

As stated in the Introduction, the $n_O \rightarrow \sigma^*_{C-O}$ hyperconjugation has been rationalized by shorter O−C bonds in the gauche conformation.[4] In the $g^+tg^+t$ conformation of PMO-3, the O2−C3 (1.385 Å) and O4−C5 (1.384 Å) bonds in the gauche state are shorter than C3−O4

(1.427 Å) and C5−O6 (1.414 Å) in trans one. The similar tendency can also be seen for the $g^+tg^+t$ conformer of PMS-3; the gauche S−C bonds are 1.819 and 1.825 Å long, and the trans bonds are 1.847 and 1.841 Å long. On average, the gauche bonds are shorter than the trans ones by 2.5% in PMO-3 but by only 1.2% in PMS-3. The gauche stability of polythioacetal may come partly from the favorable (antiparallel) dipole−dipole interaction and the $n_S \rightarrow \sigma^*_{C-S}$ hyperconjugation occurring in the gauche conformation. It should be emphasized that the flexibility of sulfur electrons reducing the S···S repulsion and unfavorable (parallel) dipole−dipole interaction in the trans conformation is a most significant feature of polythioacetal. Nevertheless, $\mu^{BOND}$'s of PMS-3 are in fairly good agreement with $\mu^{MO}$'s.

## 4. Summary

Conformational analysis of PMS and its oligomeric model compounds has been carried out by $^{13}C$ NMR experiments, ab initio MO calculations, and the RIS calculations. The results have been discussed by comparison with those for PMO and its oligomers. The first-order interaction energy $E_\sigma$ of PMS-2 in the gas phase and solutions was evaluated by dihedral angle dependence of vicinal C−H coupling constants: for example, $-1.43 \pm 0.01$ kcal mol$^{-1}$ (gas phase at 180 °C and 3.6 atm); $-1.21$ kcal mol$^{-1}$ (cyclohexane at 25 °C); $-1.05$ kcal mol$^{-1}$ (benzene at 25 °C); $-0.98$ kcal mol$^{-1}$ (chloroform at 25 °C); $-0.98$ kcal mol$^{-1}$ (methanol at 25 °C); $-0.96$ kcal mol$^{-1}$ (dimethyl sulfoxide at 25 °C). The $E_\sigma$ value ($-1.38$ kcal mol$^{-1}$) obtained from the MO calculations at the B3LYP/6-311+G(2d,p)//B3LYP/6-31G(d) level for gaseous PMS-2 at 180 °C and 3.6 atm was in good agreement with the experiment. The gauche stability of the C−S bond tends to decrease with increasing polarity of solvent. Our ab initio MO calculations showed that the conformational energy $E_\sigma$ of the PMO oligomers has chain length dependence: dimer, $-2.15$ kcal mol$^{-1}$; trimer, $-1.72$ kcal mol$^{-1}$; tetramer, $-1.6$ kcal mol$^{-1}$. In addition, the outer C−O bonds have smaller $E_\sigma$ values than the inner ones. In contrast, the PMS oligomers do not exhibit these tendencies.

The characteristic ratio and dipole moment ratio and configurational entropy of PMS of $x = 300$ were calculated to be 7.6 (9.2), 0.17 (0.091), and 3.4 (3.1) cal mol$^{-1}$ K$^{-1}$, respectively. Here, the values in the parentheses represent the corresponding quantities of PMO of $x = 300$. Thus, unperturbed PMS would be more flexible than PMO. The difference in melting point between PMS (245 °C) and PMO (180 °C) was suggested to stem from that in the enthalpy factor.

By comparison of the geometrical parameters and atomic charges and electron density distributions of PMS-3 and PMO-3, the gauche preference of the thioacetals was indicated to come partly from the antiparallel dipole−dipole interaction and the $n_S \rightarrow \sigma^*_{C-S}$ hyperconjugation formed in the gauche conformation. Sulfur electrons are so flexible as to reduce the unfavorable (parallel) dipole−dipole interaction and steric S···S repulsion occurring in the trans state. This electron flexibility, which has not been found for polyacetal, is a most noticeable characteristic of polythioacetal.

**Acknowledgment.** We thank Dr.Minamikawa of AIST for help in NMR measurements for gaseous PMS-2-$^{13}C$, Dr.Yatabe of AIST, and Dr. Mino, Professor Akutsu, and Ms. Inoki of Chiba University for valuable advice on the sample preparation, Dr. Seki of Chiba University, and Dr. Law of Imperial College for helpful advice on NMR measurements.

## References and Notes

(1) Edward, J. T. *Chem. Ind. (London)* **1955**, 1102.
(2) Lemieux, R. U.; Pavia, A. A.; Martin, J. C.; Watanabe, K. A. *Can. J. Chem.* **1969**, *47*, 4427.
(3) Kirby, A. J. *The Anomeric Effect and Related Stereoelectronic Effects at Oxygen*; Springer-Verlag: Berlin, 1983.
(4) Juaristi, E.; Cuevas, G. *The Anomeric Effect*; CRC Press: Boca Raton, FL, 1995.
(5) Altona, C.; Knobler, C.; Romers, C. *Acta Crystallogr.* **1963**, *16*, 1217.
(6) Eliel, E. L.; Giza, C. A. *J. Org. Chem.* **1968**, *33*, 3754.
(7) Romers, C.; Altona, C.; Buys, H. R.; Havinga, E. *Top. Stereochem.* **1969**, *4*, 39.
(8) Hilling, K. W., II; Lattimer, R. P.; Kuczkowski, R. L. *J. Am. Chem. Soc.* **1982**, *104*, 988.
(9) LaBarge, M. S.; Keul, H.; Kuczkowski, R. L.; Wallasch, M.; Cremer, D. *J. Am. Chem. Soc.* **1988**, *110*, 2081.
(10) Nadar, F. W.; Eliel, E. L. *J. Am. Chem. Soc.* **1970**, *92*, 3050.
(11) Juaristi, E.; Tapia, J.; Mendez, R. *Tetrahedron* **1986**, *42*, 1253.
(12) Salzner, U.; Schleyer, P. v. R. *J. Am. Chem. Soc.* **1993**, *115*, 10231.
(13) Hay, A. S.; Ding, Y. In *Polymer Data Handbook*; Mark, J. E., Ed.; Oxford University Press: New York, 1999; p 650.
(14) Iguchi, M. *Makromol. Chem.* **1976**, *177*, 549.
(15) Uchida, T.; Tadokoro, H. *J. Polym. Sci., Part A-2: Polym. Phys.* **1967**, *5*, 63.
(16) Flory, P. J.; Mark, J. E. *Makromol. Chem.* **1964**, *75*, 11.
(17) Flory, P. J. *Statistical Mechanics of Chain Molecules*; Interscience: New York, 1969.
(18) Abe, A.; Mark, J. E. *J. Am. Chem. Soc.* **1976**, *98*, 6468.
(19) Miyasaka, T.; Kinai, Y.; Imamura, Y. *Makromol. Chem.* **1981**, *182*, 3533.
(20) Smith, G. D.; Jaffe, R. L.; Yoon, D. Y. *J. Phys. Chem.* **1994**, *98*, 9072.
(21) Smith, G. D.; Jaffe, R. L.; Yoon, D. Y. *J. Phys. Chem.* **1994**, *98*, 9078.
(22) Carazzolo, G.; Valle, G. *Makromol. Chem.* **1966**, *90*, 66.
(23) Lal, J. *J. Org. Chem.* **1961**, *26*, 971.
(24) Gipstein, E.; Wellisch, E.; Sweeting, O. J. *J. Polym. Sci., Part B: Polym. Lett.* **1963**, *1*, 237.
(25) Russo, M.; Mortillaro, L.; De Checchi, C.; Valle, G.; Mammi, M. *J. Polym. Sci., Part B: Polym. Lett.* **1965**, *3*, 501.
(26) Welsh, W. J.; Mark, J. E.; Guzman, J.; Riande, E. *Makromol. Chem.* **1982**, *183*, 2565.
(27) de la Penã, J. L.; Riande, E.; Guzmán, J. *Macromolecules* **1985**, *18*, 2739.
(28) Partly based on: Fehér, F.; Vogelbruch, K. *Beiträge zur Chemie des Schwefels* **1958**, *91*, 996.
(29) Seebach, D.; Beck, A. K. *Org. Synth.* **1971**, *51*, 39.
(30) Frisch, M. J.; Trucks, G. W.; Schlegel, H. B.; Scuseria, G. E.; Robb, M. A.; Cheeseman, J. R.; Zakrzewski, V. G.; Montgomery, J. A., Jr.; Stratmann, R. E.; Burant, J. C.; Dapprich, S.; Millam, J. M.; Daniels, A. D.; Kudin, K. N.; Strain, M. C.; Farkas, O.; Tomasi, J.; Barone, V.; Cossi, M.; Cammi, R.; Mennucci, B.; Pomelli, C.; Adamo, C.; Clifford, S.; Ochterski, J.; Petersson, G. A.; Ayala, P. Y.; Cui, Q.; Morokuma, K.; Malick, D. K.; Rabuck, A. D.; Raghavachari, K.; Foresman, J. B.; Cioslowski, J.; Ortiz, J. V.; Stefanov, B. B.; Liu, G.; Liashenko, A.; Piskorz, P.; Komaromi, I.; Gomperts, R.; Martin, R. L.; Fox, D. J.; Keith, T.; Al-Laham, M. A.; Peng, C. Y.; Nanayakkara, A.; Gonzalez, C.; Challacombe, M.; Gill, P. M. W.; Johnson, B. G.; Chen, W.; Wong, M. W.; Andres, J. L.; Head-Gordon, M.; Replogle, E. S.; Pople, J. A. *Gaussian 98*, revision A.7; Gaussian, Inc.: Pittsburgh, PA, 1998.
(31) Foresman, J. B.; Frisch, Æ. *Exploring Chemistry, with Electronic Structure Methods*, 2nd ed.; Gaussian, Inc.: Pittsburgh, PA, 1996.
(32) Wong, M. W. *Chem. Phys. Lett.* **1996**, *256*, 391.
(33) Besler, B. H.; Merz, K. M., Jr.; Kollman, P. A. *J. Comput. Chem.* **1990**, *11*, 431.
(34) Singh, U. C.; Kollman, P. A. *J. Comput. Chem.* **1984**, *5*, 129.
(35) The vapor pressure of PMS-2 at 453 K was calculated as follows. Enthalpy of vaporization ($\Delta H_{vap}$) was calculated from Trouton's rule: $\Delta H_{vap}/T_{bp} \simeq 85$ J mol$^{-1}$K$^{-1}$, where $T_{bp}$ is the boiling point (420 K) of PMS-2 at 1 atm. The substitution of the $\Delta H_{vap}$ value into the Clausius−Clapeyron equation gave

a vapor pressure of 2.1 atm. Therefore, the pressure in the NMR sample tube was estimated as 3.6 atm (the vapor (2.1 atm) and atmospheric (1.5 atm at 453 K) pressures).
(36) Brant, D. A.; Miller, W. G.; Flory, P. J. *J. Mol. Biol.* **1967**, *23*, 47.
(37) Tonelli, A. *J. Chem. Phys.* **1970**, *52*, 4749.
(38) Tonelli, A. *J. Chem. Phys.* **1970**, *53*, 4339.
(39) Mark, J. E. *J. Chem. Phys.* **1977**, *67*, 3300.
(40) Abe, A. *Macromolecules* **1980**, *13*, 546.
(41) As shown in Figure 2, the NMR spectra observed from gaseous PMS-2-$^{13}C$ include intense noise. Thus, the peak position $\langle\omega\rangle$ was determined from $\langle\omega\rangle = \int_{\omega_0}^{\omega_1}\omega I(\omega)\,d\omega/\int_{\omega_0}^{\omega_1} I(\omega)\,d\omega$, where $\omega_0$ and $\omega_1$ stand for the beginning and end of the peak, and $I(\omega)$ is the intensity at a frequency $\omega$. The $^3J_{CH}$ values obtained from the four triplets were averaged, and the error margin represents the standard deviation.
(42) Abe, A.; Inomata, K.; Tanisawa, E.; Ando, I. *J. Mol. Struct.* **1990**, *238*, 315.
(43) Uchida, T.; Kurita, Y.; Kubo, M. *J. Polym. Sci.* **1956**, *19*, 365.
(44) Sakakibara, M.; Yonemura, Y.; Matsuura, H.; Murata, H. *J. Mol. Struct.* **1980**, *66*, 333.
(45) Abe, A. *Macromolecules* **1980**, *13*, 541.
(46) Riande, E.; Saiz, E. *Dipole Moments and Birefringence of Polymers*; Prentice Hall: Englewood Cliffs, NJ, 1992.
(47) Conformational energies (kcal mol$^{-1}$) $E_\sigma = -1.5$ and $E_\omega = 1.8$, bond length (Å) C−O = 1.43, bond angles (deg) ∠COC = ∠OCO = 110.0, and dihedral angles (deg) $\phi_{trans} = 0.00$ and $\phi_{gauche\pm} = \pm 120.0$. Reference 17.
(48) Conformational energies (kcal mol$^{-1}$) $E_\sigma = -1.4$ and $E_\omega = 1.5$, bond length (Å) C−O = 1.42, bond angles (deg) ∠COC = ∠OCO = 112.0, and dihedral angles (deg) $\phi_{trans} = 0.00$ and $\phi_{gauche\pm} = \pm 115.0$. Reference 18.
(49) Extrapolated value from osmotic pressure and viscosity data for PMO in phenol at 90 °C: Kokle, V.; Billmeyer, F. W., Jr. *J. Polym. Sci., Part B* **1965**, *3*, 47 and ref 17.
(50) Extrapolated value from light scattering and viscosity data for PMO in a mixed solvent of hexafluoroaceton and water at 25 °C: Stockmayer, W. H.; Chan, L. L. *J. Polym. Sci., Part A-2: Polym. Phys.* **1966**, *4*, 437.
(51) Equation 1 gives the configurational entropy in the unit of cal (mol of skeletal bond)$^{-1}$ K$^{-1}$. For comparison with experiment, however, the unit of entropy is transformed here to cal mol$^{-1}$ K$^{-1}$, which denotes cal (mol of monomer unit)$^{-1}$ K$^{-1}$.
(52) Billmeyer, F. W., Jr. *Textbook of Polymer Science*; Wiley: New York, 1962; p 161.
(53) Starkweather, H. W., Jr.; Boyd, R. H. *J. Phys. Chem.* **1960**, *64*, 410.
(54) Inoue, M. *J. Polym. Sci., Part A* **1963**, *1*, 2697.
(55) The change $\Delta S_{conf}$ in configurational entropy on melting is defined by $\Delta S_{conf} = S_{conf,a} - S_{conf,c}$, where $S_{conf,a}$ and $S_{conf,c}$ are the configurational entropies for amorphous (molten) and crystalline states, respectively. Because $S_{conf,c}$ is null, $\Delta S_{conf}$ corresponds to $S_{conf,a}$, which can be calculated from eq 1 using the conformational energies for the $\theta$ state.
(56) Kirshenbaum, I. *J. Polym. Sci., Part A* **1965**, *3*, 1869.
(57) Bhaumik, D.; Mark, J. E. *Macromolecules* **1981**, *14*, 162.
(58) Bondi, A. *J. Phys. Chem.* **1964**, *68*, 441.
(59) Pauling, L. *The Nature of the Chemical Bond and the Structure of Molecules and Crystals: An Introduction to Modern Structural Chemistry*, 3rd ed.; Cornell University Press: Ithaca, NY, 1960.

MA0109525